

23 Jun 2009

arXiv:0906.4229v1 [physics.atom-ph]

# Laser-induced nonsequential double ionization: kinematic constraints for the recollision-excitation-tunneling mechanism

T. Shaaran and C. Figueira de Morisson Faria

Department of Physics and Astronomy, University College London, Gower Street,  
London WC1E 6BT, United Kingdom

(Received 00 Month 200x; In final form 00 Month 200x)

We investigate the physical processes in which an electron, upon return to its parent ion, promotes a second electron to an excited state, from which it subsequently tunnels. Employing the strong-field approximation and saddle-point methods, we perform a detailed analysis of the dynamics of the two electrons, in terms of quantum orbits, and delimit constraints for their momentum components parallel to the laser-field polarization. The kinetic energy of the first electron, upon return, exhibits a cutoff slightly lower than  $10U_p$ , where  $U_p$  is the ponderomotive energy, as in rescattered above-threshold ionization (ATI). The second electron leaves the excited state in a direct ATI-like process, with the maximal energy of  $2U_p$ . We also compute electron-momentum distributions, whose maxima agree with our estimates and with other methods.

## 1 Introduction

Electron-electron correlation in strong laser fields has attracted a great deal of attention for over a decade, in particular in the context of laser-induced nonsequential double and multiple ionization [1]. For these specific phenomena, the electron-electron interaction plays a huge role. A concrete example are the peaks in the electron momentum distributions in nonsequential double ionization (NSDI), as functions of the electron components  $p_{n\parallel}$  ( $n = 1, 2$ ) parallel to the laser-field polarization [2]. Such peaks occur at nonvanishing parallel momenta and cannot be explained by a sequential mechanism. Whilst it is agreed upon that NSDI owes its existence to the inelastic recollision of an electron with its parent ion, there exist several open questions related to this recollision, such as the combined effect of the residual ionic potential, the electron-electron interaction and the strong laser fields on the electron-momentum distributions [3, 6, 8, 9, 7].

For instance, it can happen that the first electron, upon return, provides the second electron with enough energy so that it is able to overcome the binding energy of the singly ionized ion and reach the continuum. In this case, the second electron is released by electron-impact ionization. Both electrons leave

simultaneously and lead to distributions peaked at nonvanishing momenta, in the first and third quadrant of the plane  $p_{1\parallel}p_{2\parallel}$  spanned by the parallel momentum components. This particular rescattering mechanism has been extensively investigated in the past few years, possibly for the following reasons. First, it explained the dramatic features observed experimentally in the electron momentum distributions, namely the peaks near the non-vanishing momenta  $p_{1\parallel} = p_{2\parallel} = \pm 2\sqrt{U_p}$ , where  $U_p$  is the ponderomotive energy, and the V-shaped structure observed in the electron momentum distributions, which is a signature of the long-range character of the electron-electron interaction [3, 6, 9, 7]. Second, especially in the context of semi-analytic methods such as the strong-field approximation, electron-impact ionization is easier to model than the other rescattering mechanisms.

In the past few years, however, there has been increasing interest in below-threshold intensities, for which the kinetic energy of the recolliding electron is not sufficient to release a second electron by electron-impact ionization [8, 9]. In the below-threshold regime, the second electron is promoted to an excited bound state, from which it subsequently tunnels. This mechanism is known as the recollision-excitation-tunneling ionization (RESI). Thereby, there is a time delay between the ionization of the first and second electrons. While the first electron will rescatter near a crossing of the driving field, the second electron is expected to leave a quarter of a cycle later, i.e., near a field maximum. Since in this case both electrons are expected to reach the detector with opposite momenta, one anticipates that the second and fourth quadrant of the plane  $p_{1\parallel}p_{2\parallel}$  will be populated. Apart from the below-threshold scenario, RESI is also present to a great extent in species such as argon and helium [4, 5]. Furthermore, recent experiments and computations involving aligned molecules suggest that RESI plays an important role in this case [10, 11, 12, 13].

Up to the present moment, however, there have been relatively few studies of this specific physical mechanism, mainly in the context of classical or semiclassical methods [11, 12, 13]. Indeed, in many studies of NSDI below the threshold, electron-impact ionization has been considered instead, either in the framework of the strong-field Coulomb eikonal approximation [9], or in the context of a classical model with a modified second ionization threshold [8].

In this paper, we model this physical mechanism within the strong-field approximation (SFA). In this specific framework, the pertaining transition amplitude is written in terms of a semiclassical action and slowly varying prefactors. Employing saddle-point methods, it is possible to relate the solutions of the saddle-point equations to the classical trajectories of an electron rescattering with its parent ion and, yet, retain quantum mechanical features such as interference or excitation. This work is organized as follows: In Sec. 2, we will give the SFA transition amplitude for the RESI mechanism, which will be solved by saddle-point methods. The saddle-point equations obtained will

then be analyzed in detail, and, subsequently (Sec. 3), we will provide momentum constraints for the first and second electron. In Sec. 4, these constraints will then be tested against the electron momentum distributions. Finally, in Sec. 5 we will conclude the paper with a few summarizing remarks.

## 2 Transition amplitude

### 2.1 General expressions

The transition amplitude describing the recollision-excitation-tunneling ionization (RESI) physical mechanism reads

$$M = \int_{-\infty}^{\infty} dt \int_{-\infty}^t dt'' \int_{-\infty}^{t'} dt''' \quad (1)$$

$$\langle \mathbf{p}_1(t), \mathbf{p}_2(t) | \tilde{V}_{\text{ion}} \tilde{U}(t, t''') V_{12} U(t'', t') \tilde{V} | \psi_g^{(1)}(t'), \psi_g^{(2)}(t') \rangle,$$

where  $U(t'', t')$  and  $\tilde{U}(t'', t')$  denote the time evolution operator of the two-electron system,  $|\psi_g^{(1)}(t'), \psi_g^{(2)}(t') \rangle$  is the two-electron initial state, and  $|\mathbf{p}_1(t), \mathbf{p}_2(t)\rangle$  the final two-electron continuum state. The interactions  $\tilde{V} = P_{cg} V P_{gg}$ ,  $V_{12}$ , and  $\tilde{V}_{\text{ion}} = P_{cc} V_{\text{ion}} P_{ce}$  correspond to the atomic binding potential, the electron-electron interaction and the binding potential of the singly ionized core, respectively. We assume that the system is initially in a product state of one-electron ground states, i.e.,  $|\psi_g^{(1)}(t'), \psi_g^{(2)}(t') \rangle = |\psi_g^{(1)}(t') \rangle \otimes |\psi_g^{(2)}(t') \rangle$ , with  $|\psi_g^{(n)}(t') \rangle = \exp[iE_{ng}t'] |\varphi_g^{(n)} \rangle$ . We consider the length gauge and atomic units throughout.

The operators  $P_{\mu\nu}$  are projectors onto the bound or continuum subspaces. Specifically,

$$P_{gg} = \left| \varphi_g^{(1)}, \varphi_g^{(2)} \right\rangle \left\langle \varphi_g^{(1)}, \varphi_g^{(2)} \right| \quad (2)$$

is the projector onto the two-electron field-free ground state,

$$P_{cg} = \left| \mathbf{k}, \varphi_g^{(2)} \right\rangle \left\langle \mathbf{k}, \varphi_g^{(2)} \right| \quad (3)$$

projects the first electron onto the continuum state  $|\mathbf{k}\rangle$ , and keeps the second electron in the ground state  $|\varphi_g^{(2)}\rangle$ ,

$$P_{ce} = \left| \mathbf{k}, \varphi_e^{(2)} \right\rangle \left\langle \mathbf{k}, \varphi_e^{(2)} \right| \quad (4)$$

projects the first electron onto the continuum state  $|\mathbf{k}\rangle$ , the second electron onto the excited state  $|\varphi_e^{(2)}\rangle$ , and

$$P_{cc} = |\mathbf{k}_1, \mathbf{k}_2\rangle \langle \mathbf{k}_1, \mathbf{k}_2|. \quad (5)$$

They guarantee that the continuum and bound states remain orthogonal. For the exact time evolution operators, this property holds. The bound-continuum orthogonality is lost, however, if the continuum states are approximated by Volkov states. This is one of the key assumptions within the strong-field approximation. For details see, e.g., [14].

The time-evolution operator of the system from the tunneling time  $t'$  of the first electron to the recollision time  $t''$  was approximated by  $U(t'', t') = U_V^{(1)}(t'', t') \otimes U_g^{(2)}(t'', t')$ , where  $U_V^{(1)}$  is the Gordon-Volkov time-evolution operator for the first electron and  $U_g^{(2)}$  is the field-free time evolution operator for the second electron in the ground state. Subsequently to the recollision, the time evolution operator of the system was taken to be  $\tilde{U}(t, t'') = U_V^{(1)}(t, t'') \otimes U_e^{(2)}(t, t'')$ , where  $U_V^{(1)}$  is the Gordon-Volkov time-evolution operator for the first electron and  $U_e^{(2)}$  is the field-free time evolution operator for the second electron in the excited state of the singly ionized ion. In particular the latter assumptions, which are the neglect of the residual binding potential when the electron is in the continuum and of the laser field when the electron is bound characterize the strong-field approximation, or Keldysh-Faisal-Reiss theory.

By employing closure relations and the explicit expressions for the Gordon-Volkov time-evolution operators, Eq. (1) can be written as

$$M = \int_{-\infty}^{\infty} dt \int_{-\infty}^t dt'' \int_{-\infty}^{t'} dt''' \int d^3k V_{\mathbf{p}_2 e} V_{\mathbf{p}_1 e, \mathbf{k}g} V_{\mathbf{k}g} \exp[iS(\mathbf{p}_n, \mathbf{k}, t, t', t'')] \quad (6)$$

with the action

$$\begin{aligned} S(\mathbf{p}_n, \mathbf{k}, t, t', t'') = & - \int_t^{\infty} d\tau \frac{[\mathbf{p}_2 + \mathbf{A}(\tau)]^2}{2} - \int_{t''}^{\infty} d\tau \frac{[\mathbf{p}_1 + \mathbf{A}(\tau)]^2}{2} \\ & - \int_{t'}^{t''} d\tau \frac{[\mathbf{k} + \mathbf{A}(\tau)]^2}{2} + E_{2e}(t - t'') \\ & + E_{2g}t'' + E_{1g}t'. \end{aligned} \quad (7)$$

Thereby,  $\mathbf{A}(\tau)$  is the vector potential, the energy  $E_{1g}$  denotes the first ionization potential,  $E_{2g}$  the ground-state energy of the singly ionized atom and  $E_{2e}$

the energy of the state to which the second electron is excited. The intermediate momentum of the first electron is given by  $\mathbf{k}$  and the final momenta of both electrons by  $\mathbf{p}_n$  ( $n = 1, 2$ ). Eq. (6) describes a physical process in which the first electron leaves the atom at a time  $t'$ , propagates in the continuum with momentum  $\mathbf{k}$  from  $t'$  to  $t''$ , and upon return, gives part of the kinetic energy to the core so that a second electron is promoted from a state with energy  $E_{2g}$  to an excited state with energy  $E_{2e}$ . This electron then reaches the detector with momentum  $\mathbf{p}_1$ . At a subsequent time  $t$ , the second electron tunnels from the excited state, reaching the detector with momentum  $\mathbf{p}_2$ .

Within our framework, all influence of the electron-electron interaction and of the binding potential is contained in the prefactors  $V_{\mathbf{p}_2e}$ ,  $V_{\mathbf{p}_1e,\mathbf{k}g}$  and  $V_{\mathbf{k}g}$ . Explicitly, they read

$$V_{\mathbf{p}_2e} = \langle \mathbf{p}_2(t) | V_{\text{ion}} | \varphi_e^{(2)} \rangle = \frac{1}{(2\pi)^{3/2}} \int d^3r_2 V_{\text{ion}}(\mathbf{r}_2) e^{-i\mathbf{p}_2(t)\cdot\mathbf{r}_2} \varphi_e^{(2)}(\mathbf{r}_2), \quad (8)$$

$$V_{\mathbf{p}_1e,\mathbf{k}g} = \left\langle \mathbf{p}_1(t''), \varphi_e^{(2)} \left| V_{12} \right| \mathbf{k}(t''), \varphi_g^{(2)} \right\rangle = \frac{1}{(2\pi)^3} \int \int d^3r_2 d^3r_1 e^{-i(\mathbf{p}_1-\mathbf{k})\cdot\mathbf{r}_1} \left[ \varphi_e^{(2)}(\mathbf{r}_2) \right]^* \varphi_g^{(2)}(\mathbf{r}_2) V_{12}(\mathbf{r}_1, \mathbf{r}_2) \quad (9)$$

and

$$V_{\mathbf{k}g} = \langle \mathbf{k}(t') | V | \varphi_g^{(1)} \rangle = \frac{1}{(2\pi)^{3/2}} \int d^3r_1 e^{-i\mathbf{k}(t')\cdot\mathbf{r}_1} V(\mathbf{r}_1) \varphi_g^{(1)}(\mathbf{r}_1), \quad (10)$$

where  $\mathbf{k}(\tau) = \mathbf{k} + \mathbf{A}(\tau)$  and  $\mathbf{p}_n(\tau) = \mathbf{p}_n + \mathbf{A}(\tau)$ ,  $\tau = t, t', t''$ . In the above-stated equations,  $\varphi_e^{(2)}(\mathbf{r}_2)$ ,  $\varphi_g^{(2)}(\mathbf{r}_2)$ , and  $\varphi_g^{(1)}(\mathbf{r}_1)$  denote the initial position-space wave functions of the second electron in the excited state, of the second electron in the ground state and of the first electron in the ground state, respectively. The potentials  $V(\mathbf{r}_1)$  and  $V_{\text{ion}}(\mathbf{r}_2)$  correspond to the atomic binding potential as seen by the first and second electron, respectively. One should note that the form factor  $V_{\mathbf{p}_2e}$  is formally identical that obtained for direct above-threshold ionization, in which an electron, initially bound, reaches the detector without rescattering [15].

Under the additional assumption that the electron-electron interaction depends only on the difference between the two electron coordinates, i.e.,  $V_{12}(\mathbf{r}_1, \mathbf{r}_2) = V_{12}(\mathbf{r}_1 - \mathbf{r}_2)$ , Eq. (9) may be written as

$$V_{\mathbf{p}_1e,\mathbf{k}g} = \frac{V_{12}(\mathbf{p}_1-\mathbf{k})}{(2\pi)^3} \int d^3r_2 e^{-i(\mathbf{p}_1-\mathbf{k})\cdot\mathbf{r}_2} \left[ \varphi_e^{(2)}(\mathbf{r}_2) \right]^* \varphi_g^{(2)}(\mathbf{r}_2), \quad (11)$$

with

$$V_{12}(\mathbf{k}(t'')) = \int d^3r V_{12}(\mathbf{r}) \exp[-i(\mathbf{p}_1 - \mathbf{k}) \cdot \mathbf{r}] \quad (12)$$

and  $\mathbf{r} = \mathbf{r}_1 - \mathbf{r}_2$ . One should note that the prefactor (11), resembles that obtained for high-order above-threshold ionization, in which an electron reaches the detector after suffering one act of rescattering [15].

## 2.2 Saddle-point analysis

In this work, we solve the transition amplitude (6) employing saddle point methods. For that purpose, one must obtain the saddle-point equations, which give the values of the variables  $\mathbf{k}, t, t'', t'$  for which the action is stationary. Explicitly, these equations are obtained from the conditions  $\partial S(\mathbf{k}, t, t'', t')/\partial t' = 0$ ,  $\partial S(\mathbf{k}, t, t'', t')/\partial t'' = 0$ ,  $\partial S(\mathbf{k}, t, t'', t')/\partial t = 0$  and  $\partial S(\mathbf{k}, t, t'', t')/\partial \mathbf{k} = \mathbf{0}$ . This gives

$$[\mathbf{k} + \mathbf{A}(t')]^2 = -2E_{1g}, \quad (13)$$

$$\mathbf{k} = -\frac{1}{t'' - t'} \int_{t'}^{t''} \mathbf{A}(\tau) d\tau, \quad (14)$$

$$[\mathbf{p}_1 + \mathbf{A}(t'')]^2 = [\mathbf{k} + \mathbf{A}(t'')]^2 - 2(E_{2g} - E_{2e}) \quad (15)$$

and

$$[\mathbf{p}_2 + \mathbf{A}(t)]^2 = -2E_{2e}. \quad (16)$$

The saddle-point equation (13) gives the conservation of energy at the instant  $t'$ . Physically, it corresponds to tunneling ionization of the first electron. Eq. (14) constrains the intermediate momentum  $\mathbf{k}$  of this electron so that it can return to its parent ion. Eq. (15) expresses the fact that the first electron returns at a time  $t''$  and gives part of its kinetic energy  $E_{\text{ret}}(t'') = [\mathbf{k} + \mathbf{A}(t'')]^2/2$  to the core, which is excited from a state with energy  $E_{2g}$  to a state with energy  $E_{2e}$ . This electron then reaches the detector with final momentum  $\mathbf{p}_1$ . Finally, a second electron tunnels from the excited state at a subsequent time  $t$ , and

reaches the detector with final momentum  $\mathbf{p}_2$ . The conservation of energy at this instant is given by the saddle-point equation (16). One should note that the saddle-point Eqs. (13) and (16) have no real solution. In both cases,  $\text{Im}[t']$  and  $\text{Im}[t]$  give a rough idea of the width of the barrier and of the ionization probability for the first and the second electron, respectively. The larger this quantity is, the wider the barrier through which they must tunnel.

In order to compute the transition amplitude, we follow the procedure discussed in [19], and employ the saddle point Eq. (14) to reduce the number of independent variables in the uniform approximation used. The main difference from [19] is that, in this paper, we deal with three independent variables, i.e.,  $t, t'$  and  $t''$ , instead of only  $t$  and  $t'$ . Apart from that, the saddle-point equation (16) is decoupled from the remaining saddle-point equations, so that the ionization time  $t$  for the second electron can be determined independently. Physically, however, we should guarantee that  $t > t'' > t'$ .

Unless stated otherwise, we consider momentum distributions for which the perpendicular momentum components  $\mathbf{p}_{n\perp}$  ( $n = 1, 2$ ) are integrated over. In the following, we will discuss which momentum regions such distributions will occupy, and the physical reasons behind it.

### 3 Constraints in momentum space

From the saddle-point equations in the previous section, one may determine constraints for the parallel momentum components  $p_{n\parallel}$  ( $n = 1, 2$ ) in the plane  $p_{1\parallel}p_{2\parallel}$ . These constraints will be discussed here, and will serve as a tool to sketch an approximate shape for the electron-momentum distributions. For simplicity, we will consider a monochromatic field of frequency  $\omega$ , i.e.,  $E(t) = -dA(t)/dt = 2\omega\sqrt{U_p}\sin\omega t$ .

Eq. (16), which corresponds to the tunneling of the second electron, is formally identical to the saddle-point equation describing the low-energy electrons in above-threshold ionization (ATI), the so-called “direct electrons”. In this case, an electron tunnels from a bound state and reaches the detector without rescattering with its parent ion.

Physically, this is exactly the situation encountered for the second electron, and will have two main consequences. Firstly, the solutions of the saddle-point equations will be identical to those for the direct ATI electrons [16]. For vanishing electron drift momenta, these solutions are displaced by half a cycle, and are located at a maximum of the field. As the momentum increases, the solutions approach each other and move away from the maximum. Secondly, the maximal kinetic energy for the direct ATI electrons is  $2U_p$ . Hence, if the perpendicular components vanish, we will have an upper and lower bound for  $p_{2\parallel}$ . Explicitly,  $-2\sqrt{U_p} \leq p_{2\parallel} \leq 2\sqrt{U_p}$ . One should note that this in contrast

to the situation discussed in our previous papers [3, 18], in which the second electron is dislodged by electron-impact ionization. In this latter case,  $\pm 2\sqrt{U_p}$  is the *most probable* momentum  $p_{2\parallel}$  with which the second electron may leave, whereas, in the present scenario, this is the *maximum* value for this quantity. For nonvanishing transverse momenta, this region will remain the same. We expect, however, that there will be a large drop in the yield. This is due to the fact that there will be an effective increase in the potential barrier through which the electron tunnels. This can be readily verified by writing the saddle-point equation (16) as

$$[p_{2\parallel} + A(t)]^2 = -2\tilde{E}_{2e}, \quad (17)$$

with  $\tilde{E}_{2e} = E_{2e} + \mathbf{p}_{2\perp}^2/2$ .

In Fig. 1, we plot the real and imaginary parts of such times, as functions of the electron momentum  $p_{2\parallel}$ , for several transverse momenta (upper and lower panel, respectively). In all cases, the imaginary parts of each time  $t$  in a pair are identical and exhibit a minimum at the peak-field times  $\omega t = \pi/2$ . This is expected, as i) the two orbits behave symmetrically with respect to the laser field, and ii) the effective potential barrier through which the electron tunnels is narrowest for these times. As the transverse momentum  $\mathbf{p}_{2\perp}$  becomes larger in absolute value, we see an increase in  $\text{Im}[t]$ . This is consistent with the fact that the potential barrier widens in this case.

Eq. (15), on the other hand, has a similar form as the saddle-point equation describing the rescattered electrons in ATI [19], apart from the energy difference  $E_{2g} - E_{2e}$  on the right-hand side. Physically, this is somehow expected, as in both cases the first electron leaves immediately after rescattering. The difference is that, while in ATI the rescattering is elastic, in NSDI part of the electron's kinetic energy is used to excite the core. For ATI, the maximal energy with which the electron rescatters is  $10U_p$ , and corresponds to backscattered electrons. Therefore, to first approximation, this will be employed to compute the upper bound for the parallel electron momentum  $p_{1\parallel}$ . Clearly, this kinetic energy will be subtracted by  $E_{2g} - E_{2e}$  and is slightly smaller.

Apart from that, there is also a minimal energy for the first electron to excite its parent ion and still rescatter. This is given by the condition  $E_{2g} - E_{2e} = [\mathbf{k} + \mathbf{A}(t'')]^2/2$ , and implies a vanishing right-hand side on Eq. (15). For vanishing perpendicular momentum, this will lead to  $p_{1\parallel} = -A(t'')$ . Since, to first approximation, the electron returns at a field crossing, this implies that  $-2\sqrt{U_p} \lesssim p_{1\parallel} \lesssim 4\sqrt{U_p}$ . For the orbits leading to the mirror image of the distribution with respect to the reflection  $(p_{1\parallel}, p_{2\parallel}) \rightarrow (-p_{1\parallel}, -p_{2\parallel})$ , the constraint upon the parallel momentum of the first electron will be  $-4\sqrt{U_p} \lesssim p_{1\parallel} \lesssim 2\sqrt{U_p}$ . For these latter orbits, the times  $t', t''$  and  $t$  are displaced by



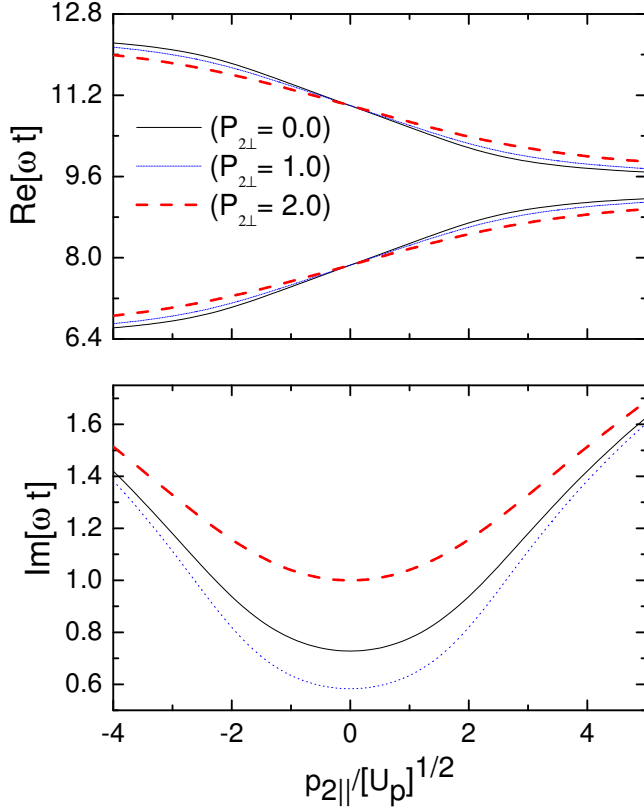


Figure 1. Tunneling time  $t$  for the second electron, as functions of its parallel momentum  $p_{2||}$ , for a monochromatic field of intensity  $I = 1.5 \times 10^{14} \text{ W/cm}^2$  and frequency  $\omega = 0.057$  a.u., for several transverse momenta  $p_{2\perp}$ . The upper and lower panel give the real and imaginary parts of such times, respectively. We consider that the second electron is promoted to the  $2p$  state of the Helium atom, from which it subsequently tunnels, i.e.,  $E_{2e} = 0.25$  a.u. and  $E_{2g} = 1$  a.u.

half a cycle. A nonvanishing transverse momentum component  $\mathbf{p}_{1\perp}$  will lead to lower maximal and minimal momenta.

In Fig. 2, we display the real and imaginary part of the ionization [panels (a) and (b), respectively] and rescattering times [panels (c) and (d), respectively] for the first electron. We consider the shortest orbits for the returning electron. The remaining sets of orbits are strongly suppressed due to wave-packet spreading. By associating the real parts of  $t'$  and  $t''$  with the classical trajectories of an electron in a laser field, one may identify a longer and a shorter orbit, along which the first electron returns. These orbits practically coalesce for two specific values of  $p_{1||}$ , namely the minimum and the maximum momenta for which the rescattering process described by the saddle-point equation (15) has a classical counterpart. Beyond these momenta, the yield decays exponentially.

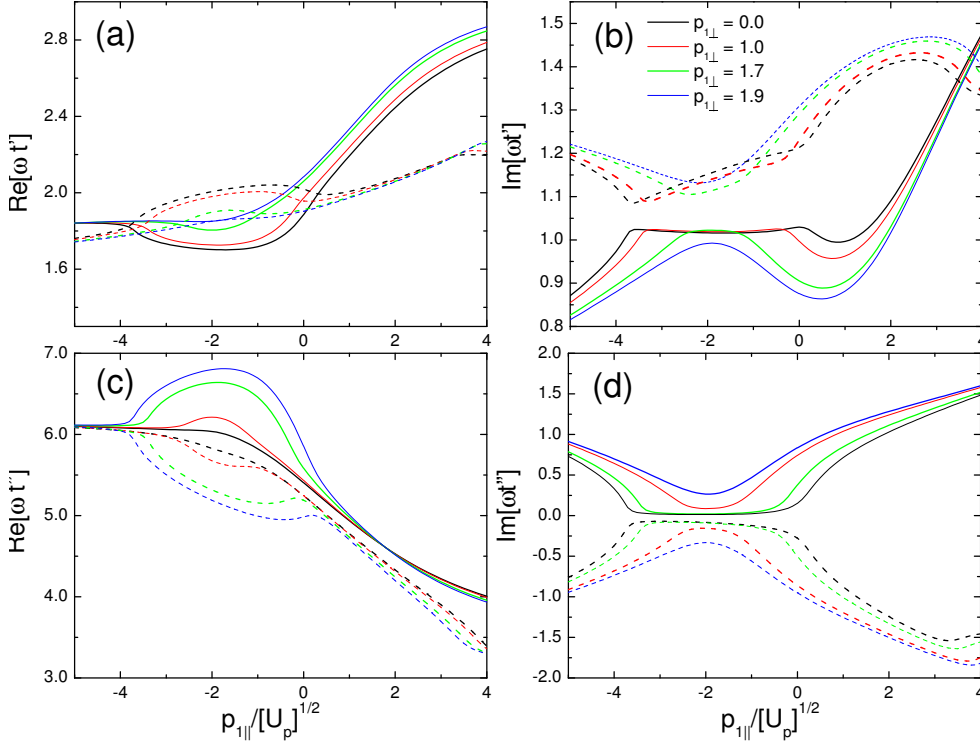


Figure 2. Tunneling and rescattering times for the first electron, as functions of its parallel momentum  $p_{1||}$ . Panels (a) and (b) give the real and imaginary parts of the tunneling time  $t'$ , respectively, and panels (c) and (d) depict the the real and imaginary parts of the rescattering time  $t''$ . We consider that the electron tunnels from the  $2s$  state of the Helium atom, i.e.,  $E_{1g} = 0.92$  a.u., and rescatters with the  $1s$  state of  $He^+$ , i.e.,  $E_{2g} = 1$  a.u. Thereby the returning electron gives part of its kinetic energy to excite a second electron to the state  $E_{2e} = 0.25$  a.u. The dashed and solid lines correspond to the short and long orbits, respectively.

For vanishing transverse momentum  $p_{1\perp}$ , these cutoffs are near  $-4\sqrt{U_p}$  and  $2\sqrt{U_p}$ , as predicted by our estimates. As  $p_{1\perp}$  increases, the classically allowed region shrinks and gets very localized near  $p_{1||} = -2\sqrt{U_p}$ . For the parameters considered here, this corresponds to the situation in which the electron returns at a crossing of the field. Finally, for very large transverse momenta, this region disappears.

The imaginary parts of the times  $t'$  and  $t''$ , displayed in Figs. 2.(b) and 2.(d), confirm this physical interpretation. In fact, they show that, for the rescattering times,  $\text{Im}[t'']$  essentially vanishes between the momenta for which the real parts  $\text{Re}[t'']$  coalesce. Physically, this means that, in this region, rescattering is classically allowed. Beyond this region,  $\text{Im}[t'']$  increases abruptly, which indicates that the classically forbidden region has been reached. In this context, it is worth mentioning that, even if there is no classically allowed region,

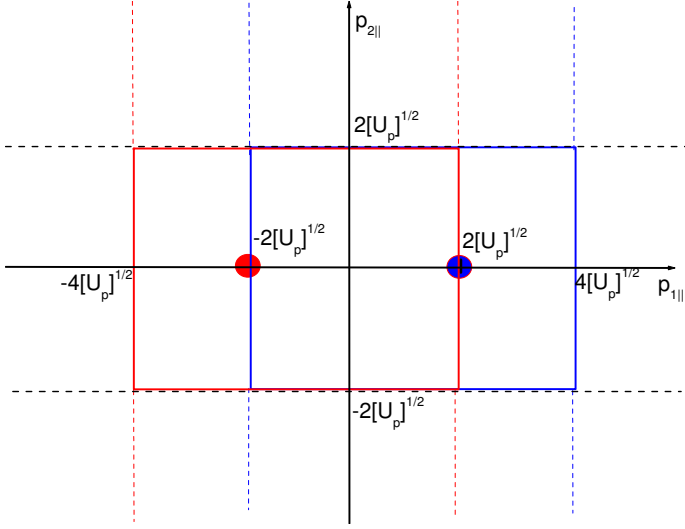


Figure 3. Schematic representation of the regions of the parallel momentum plane populated by the recollision-excitation-tunneling ionization mechanism, highlighted as the rectangles in the figure. The dashed black lines indicate the constraints in the parallel momentum  $p_{2||}$  of the second electron, while the remaining dashed lines depict the limits for the parallel momentum  $p_{1||}$  of the first electron. The circles indicate the expected maxima of the electron momentum distributions. The blue and red colors indicate different sets of trajectories, whose start and recollision times are separated by half a cycle of the field. In our estimates, we considered vanishing transverse momenta, so that the constraints provided constitute an upper bound for this region. The above plot has not been symmetrized with respect to the indistinguishability of the two electrons.

$\text{Im}[t'']$  exhibits a minimum near  $p_{1||} = -2\sqrt{U_p}$ . This is due to the fact that rescattering is most probable for this specific momentum. A similar behavior has been observed in [17] for electron-impact ionization.

The imaginary part  $\text{Im}[t']$  of the start time of the first electron, on the other hand, is always non-vanishing. This is not surprising, as tunneling has no classical counterpart. They are, however, approximately constant between the lower and upper cutoff momenta.

By solving the saddle-point Eqs. (15) and (16), we verified that, if we consider the physically relevant parameters, namely that  $t \sim t'' + T/4$ , where  $T = 2\pi/\omega$  denotes a laser-field cycle, then  $p_{2||}$  will be predominantly positive and  $p_{1||}$  will be predominantly negative. Conversely, for the orbits whose start, rescattering and tunneling times are displaced by half a cycle,  $p_{2||}$  will be mainly negative and  $p_{1||}$  will be predominantly positive. Therefore, one expects that the distributions will be mainly concentrated in the second and fourth quadrants of the parallel momentum plane.

In Fig. 3, we summarize the information discussed above, and provide a schematic representation of the momentum regions occupied in the RESI process. In particular, we expect the distributions to exhibit maxima near the

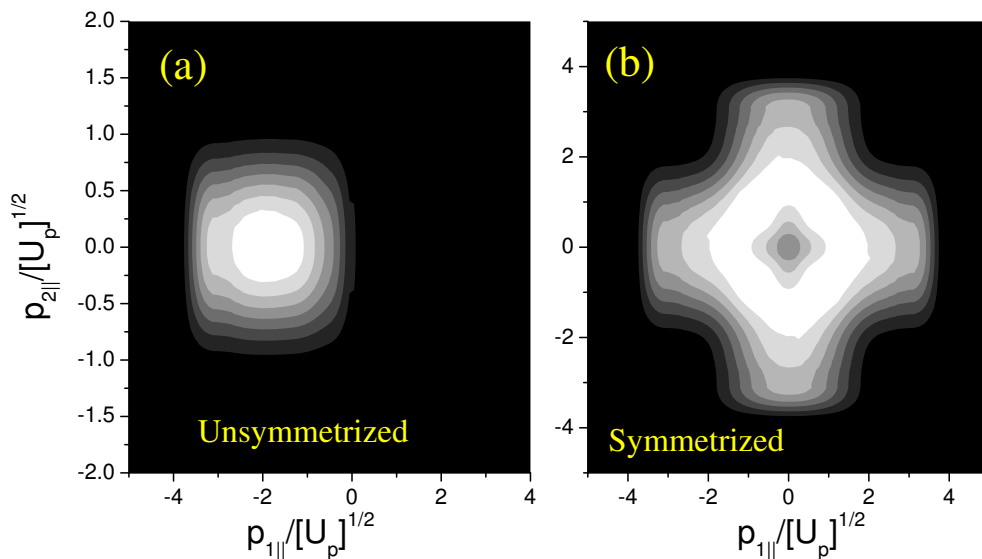


Figure 4. Electron momentum distributions for Helium ( $E_{1g} = 0.92$  a.u.,  $E_{2g} = 1$  a.u. and  $E_{2e} = 0.25$ ) in a linearly polarized, monochromatic field of frequency  $\omega = 0.057$  a.u. and intensity  $I = 1.5 \times \text{W/cm}^2$ . Panel (a) displays only the contributions from the sets of orbits starting at  $0 < t' < T/2$ , while panel (b) depicts also the contributions from the other half-cycle of the field. In panel (b), the distributions have also been symmetrized with respect to the exchange  $\mathbf{p}_1 \leftrightarrow \mathbf{p}_2$

points  $(p_{1||}, p_{2||}) = (\pm 2\sqrt{U_p}, 0)$ . In a real-life situation, since both electrons are indistinguishable, one would expect maxima also at  $(p_{1||}, p_{2||}) = (0, \pm 2\sqrt{U_p})$ .

#### 4 Electron momentum distributions

In this section, we compute electron-momentum distributions employing Eq. (6), under the assumption that the prefactors  $V_{\mathbf{p}_{2e}}, V_{\mathbf{p}_{1e}, \mathbf{k}_g}$  and  $V_{\mathbf{k}_g}$  are constant. This removes any momentum bias that may arise from such prefactors, and therefore provides a clearer picture of how the momentum-space constraints affect such distributions. The transverse momentum components are integrated over.

Fig. 4 depicts such distributions. In panel (a), we consider only that the first electron is released in  $0 < t' < T/2$ , where  $T = 2\pi/\omega$  denotes a cycle of the external driving field, while in panel (b) we also consider the contributions from  $t' \rightarrow t' \pm T/2$ ,  $t'' \rightarrow t'' \pm T/2$  and  $t \rightarrow t \pm T/2$ . Furthermore, in the latter case, we also symmetrize the distributions with respect to  $\mathbf{p}_1 \leftrightarrow \mathbf{p}_2$ , as the two electrons are indistinguishable. We have considered the parameters for Helium, corresponding to the situation in which an electron initially in  $1s$  was released and promoted a second electron to the  $2p$  state.

In Fig. 4.(a), one clearly sees that the distributions are brightest along the axis  $p_{2\parallel} = 0$ . This is expected, as the emission of the second electron is most probable at a field maximum. For this time, the electron momentum vanishes. Apart from that, the distribution is longer in the  $p_{1\parallel}$  direction. This is expected, as the cutoff momenta is higher in this case. Finally, the distributions also exhibit a maximum at  $p_{1\parallel} = -2\sqrt{U_p}$ , in agreement with the above-defined constraints. Upon symmetrization [Fig. 4.(b)], we obtain distributions highly concentrated along the momentum axis  $p_{1\parallel} = 0$  and  $p_{2\parallel} = 0$ . These distributions also exhibit a ring-shaped maximum around the origin of the  $p_{1\parallel}p_{2\parallel}$  plane. These results show that the momentum regions populated by the RESI mechanism are much lower than those populated if the second electron is released by electron-impact ionization, in agreement with other results reported in the literature [4, 5].

## 5 Conclusions

The main conclusion to be inferred from this work is that the recollision-excitation-ionization mechanism, which is becoming increasingly studied due to its importance for NSDI of molecules and at threshold intensities, can be understood as rescattered above-threshold ionization (ATI) for the first electron, followed by direct ATI for the second electron. The kinematic constraints imposed by both processes lead to cross-shaped electron momentum distributions, localized at the axis  $p_{1\parallel} = 0$  or  $p_{2\parallel} = 0$ , and centered at  $p_{1\parallel} = p_{2\parallel} = 0$ .

The fact that these distributions are concentrated in the low momentum regions is not surprising. Physically, much less energy is required to promote an electron to an excited state, from which it subsequently tunnels, than to provide the second electron with enough energy so that it may overcome the second ionization potential and reach the continuum, as in electron-impact ionization [3, 9]. Furthermore, since for the recollision-excitation-tunneling mechanism there is a time delay between the ionization of the first and second electron, the second and fourth quadrants of the plane spanned by the parallel momentum components  $p_{n\parallel}$  are populated [11, 12]. This is not the case in electron-impact ionization, for which both electrons leave simultaneously. In contrast to the results reported in [11, 12], however, we did not observe a localization of the distributions only in such regions. Such an effect is possibly due to the influence of the long-range tail of the Coulomb potential, and is presently under investigation.

**Acknowledgements** This work has been financed by the UK EPSRC (Advanced Fellowship, Grant no. EP/D07309X/1 and DTA studentship). We thank A. Emmanouilidou and M. Ivanov for useful discussions.

## References

- [1] For a review on this subject see, e.g., R. Dörner, Th. Weber, M. Weckenbrock, A. Staudte, M. Hattas, H. Schmidt-Böcking, R. Moshhammer, J. Ullrich: *Adv. At., Mol., Opt. Phys.* **48**, 1 (2002).
- [2] See e.g., Th. Weber, M. Weckenbrock, A. Staudte, L. Spielberger, O. Jagutzki, V. Mergel, F. Afaneh, G. Urbasch, M. Vollmer, H. Giessen, and R. Dörner, *Phys. Rev. Lett.* **84**, 444 (2000); R. Moshhammer, B. Feuerstein, W. Schmitt, A. Dorn, C.D. Schröter, J. Ullrich, H. Rottke, C. Trump, M. Wittmann, G. Korn, K. Hoffmann, and W. Sandner, *Phys. Rev. Lett.* **84**, 447 (2000) for key experiments on the subject.
- [3] C. Figueira de Morisson Faria, H. Schomerus, X. Liu, and W. Becker, *Phys. Rev. A* **69**, 043405 (2004); C. Figueira de Morisson Faria, and M. Lewenstein, *J. Phys. B* **38**, 3251 (2005).
- [4] V.L.B. de Jesus, B. Feuerstein, K. Zrost, D. Fischer, A. Rudenko, F. Afaneh, C.D. Schröter, R. Moshhammer, and J. Ullrich, *J. Phys. B* **37**, L161 (2004).
- [5] R. Kopold, W. Becker, H. Rottke and W. Sandner, *Phys. Rev. Lett.* **85**, 3871 (2000).
- [6] A. Emmanouilidou, *Phys Rev A* **78**, 023411 (2008); D. F. Ye, X. Liu, and J. Liu, *Phys. Rev. Lett.* **101**, 233003 (2008).
- [7] J. S. Prauzner-Bechcicki, K. Sacha, B. Eckhardt, and J. Zakrzewski, *Phys. Rev. A* **78**, 013419 (2008).
- [8] E. Eremina, X. Liu, H. Rottke, W. Sandner, A. Dreischuch, F. Lindner, F. Grasbon, G.G. Paulus, H. Walther, R. Moshhammer, B. Feuerstein, and J. Ullrich, *J. Phys. B.* **36**, 3269 (2003); E. Eremina, X. Liu, H. Rottke, W. Sandner, M. G. Schätzel, A. Dreischuh, G. G. Paulus, H. Walther, R. Moshhammer, and J. Ullrich, *Phys. Rev. Lett.* **92**, 173001 (2004); Yunquan Liu, S. Tschuch, A. Rudenko, M. Dürr, M. Siegel, U. Morgner, R. Moshhammer, and J. Ullrich, *Phys. Rev. Lett.* **101**, 053001 (2008).
- [9] Denys I. Bondar, Wing-Ki Liu, and Misha Yu. Ivanov, *Phys. Rev. A* **79**, 023417 (2009).
- [10] D. Zeidler, A. Staudte, A. B. Bardon, D. M. Villeneuve, R. Dörner, and P. B. Corkum, *Phys. Rev. Lett.* **95**, 203003 (2005); D. F. Ye, J. Chen, and J. Liu, *Phys. Rev. A* **77**, 013403 (2008).
- [11] J. S. Prauzner-Bechcicki, K. Sacha, B. Eckhardt, and J. Zakrzewski, *Phys. Rev. A* **71**, 033407 (2005).
- [12] Y. Li, J. Chen, S. P. Yang, and J. Liu, *Phys. Rev. A* **76**, 023401 (2007); D. F. Ye, J. Chen, and J. Liu, *Phys. Rev. A* **77**, 013403 (2008).
- [13] S. Baier, A. Becker and L. Plaja, *Phys. Rev. A* **78**, 013409 (2008).
- [14] O. Smirnova, M. Spanner and M. Ivanov, *J. Mod. Opt.* **54**, 1019 (2007).
- [15] W. Becker, A. Lohr, M. Kleber and M. Lewenstein, *Phys. Rev. A* **56**, 645 (1997).
- [16] R. Kopold, PhD thesis, Technical University Munich, 2001.
- [17] C. Figueira de Morisson Faria and W. Becker, *Laser Phys.* **13**, 1196 (2003).
- [18] C. Figueira de Morisson Faria, T. Shaaran, X. Liu and W. Yang, *Phys. Rev. A* **78**, 043407 (2008).
- [19] C. Figueira de Morisson Faria, H. Schomerus and W. Becker, *Phys. Rev. A* **66**, 043413 (2002).